Received: 2 September 2020 | Revised: 22 October 2020 | Accepted: 3 November 2020

DOI: 10.1002/qua.26544

FULL PAPER

International Journal of QUANTUM CHEMISTRY WILEY

Partitioning of the interaction-induced polarizability of molecules in helium environments

Marta Chołuj | Bartosz Błasiak | Wojciech Bartkowiak

Department of Physical and Quantum Chemistry, Wrocław University of Science and Technology, Wrocław, Poland

Correspondence
Marta Chołuj and Bartosz Błasiak, Department of Physical and Quantum Chemistry, Wrocław University of Science and Technology, Wybrzeże Wyspiańskiego 27, PL-50370 Wrocław, Poland.
Email: marta.choluj@pwr.edu.pl (M. C.) and bartosz.blasiak@pwr.edu.pl (B. B.)

Funding information
National Science Centre, Poland, 2016/23/P/ST4/01720; H2020 Marie Skłodowska-Curie Actions, 665778

Abstract

In this study, we analyze the correspondence between the spatial confinement represented by the real chemical environment in the form of helium clusters and by the repulsive analytical potential. In doing so, we perform a decomposition of the interaction-induced polarizability of the LiH and HF molecules in various helium environments into electrostatic, exchange, repulsion and polarization contributions. The obtained results show that in the low and medium orbital compression region the behavior of the repulsion contribution to the interaction-induced polarizability of LiH and HF embedded in helium environments is in line with the behavior of the total polarizability of molecules entrapped within the repulsive confining potential.

KEYWORDS
interaction-induced polarizability, orbital compression, repulsion component, repulsive potentials, spatial confinement

1 | INTRODUCTION

The studies of spatially confined atomic and molecular systems (i.e. systems enclosed within confining chemical cages, under high pressure or in solvent environments) have been conducted on both experimental and theoretical basis for many years and it is now well established that the spatial restriction can significantly modify various chemical and physical properties.[1-3] Two main approaches used in quantum chemistry to model the spatial confinement are (a) repulsive analytical potentials[1] and (b) supermolecular method.[4-14] The repulsive potentials (e.g. harmonic oscillator potential, gaussian-type potential, impenetrable spherical box) describe only pure electronic compression and express the repulsion effects which arise from the Pauli exclusion principle (often called the orbital compression effects).[1,2,15-23] Therefore, such potentials constitute an approximate representation of the real chemical confinement. Although in reality the spatial confinement affects the system as a whole, using repulsive potentials that act directly only on electrons has a strong justification, as the exchange-repulsion of electrons is an important source of confinement especially in non-polarizable, electronically inert chemical environments.[16,24] In particular, it was shown in the paper by Sarsa and Le Sech that confining the electrons by impenetrable spherical surfaces contributes much more to the observed increase of the energy of H_2^+ than confining the nuclei.[25] On the other hand, in supermolecular approach the spatial confinement is defined explicitly in a form of some sort of molecular cage. This gives us the full picture of the behavior of spatially confined objects, however the computational cost of performing accurate analysis for such systems can be very high. It should also not be overlooked that there are other methods that allow to include the spatial confinement effects in the studies. For instance, Cammi et al proposed a new approach, based on the polarizable continuum model,[26] (called polarizable continuum model - extreme pressure, PCM-XP) that accounts for the pressure effect by changing the size of the cavity in which the studied object is placed.[27-29]

The strong influence of the spatial confinement, represented by either repulsive potentials or molecular cages, on the electronic structure and electric properties of various atomic and molecular systems has been demonstrated in a plethora of theoretical works.[4-14,16,18,20-25,30-59] The correspondence between the real chemical environment in the form of carbon nanotubes or nanotube-like and fullerene-like helium clusters and the confining harmonic oscillator potential was analyzed by Kozłowska et al[5] as well as by Kaczmarek and Bartkowiak.[8] In particular, it is important to

note that, among various molecular cages, the chemically and electronically inert ones built of weakly polarizable helium atoms can potentially serve as a good representation of the orbital compression.[8, 9] However, Kozłowska et al showed that in some cases the electric properties can display qualitatively different trends of changes, depending on whether a molecule is enclosed within the cylindrically symmetric harmonic oscillator potential or within the helium cage. A good example of this fact are the LiH and HF molecules embedded in helium nanotubes (denoted as LiH@(n,n)HeNT and HF@(n,n)HeNT, respectively), because when nanotube's diameter becomes smaller, polarizability of LiH (defined as $\alpha_{zz,diff}$ = α_{zz}(AB@(n,n)HeNT)−α_{zz}((n,n)HeNT), where in this case AB = LiH) decreases, whereas in the case of HF@(n,n)HeNTs a growth of $\alpha_{zz,diff}$ occurs.[5] In the presence of the cylindrical harmonic oscillator potential polarizability of both these molecules diminishes. In fact, it is well-known that increasing the strength of orbital compression, modeled by external repulsive potentials, always leads to a decrease of polarizability. This can be easily explained, because polarizability is proportional to the molecular volume of a chemical object, whereas confining potentials compress the electron density causing a reduction of the molecular volume, hence also of the polarizability. Therefore, polarizability constitutes a very good test case for comparing two different models of spatial confinement, i.e. real molecular cages and confining repulsive potentials.

In this communication we would like to further analyze the issue of the correspondence between the two approaches of modeling the spatial confinement by looking at the repulsion effects of the confining helium environment and comparing them to these represented by the repulsive potential. For that purpose, we perform the partitioning of the electronic interaction-induced polarizability of previously studied LiH@(n,n)HeNT and HF@(n,n)HeNT systems[5] into the exchange, repulsion, electrostatic and polarization terms and analyze the behavior of all these terms under the pressure exerted by helium nanotubes of different diameter. We also include in our analysis the six model systems, that were previously studied in the context of the influence of directional character of orbital compression on the exchange-repulsion energy as well as linear and nonlinear electric properties,[9] in which various numbers of He atoms are placed at different orientations and distances from the LiH molecule (denoted as LiH-$(He)_n$).[9] Throughout the text we are following the notations used in the original papers. At this stage it is worth mentioning that the investigations of the origins of interaction-induced electric properties by their partitioning into contributions arising from various interaction energy terms have been conducted for many years, as a precise understanding of interactions between complex's subsystems allows for conscious tuning of molecular properties with an eye towards various novel applications.[60-72] One of the first works on this subject were done by Fowler and Sadlej[60,61] as well as by Moszyński and his collaborators[62,63] back in 1990s. The studies conducted so far were focused on the analysis of electronic interaction-induced electric properties. However, more recently, Zalesny et al presented a new scheme which allows for the decomposition of not only electronic but also vibrational interaction-induced (hyper)polarizabilities.[72] In the field of spatial confinement the decomposition of the interaction-induced electric properties of LiH embedded in nanotube-like and fullerene-like helium clusters was performed by Kaczmarek and Bartkowiak.[8] As a result it was found, among other things, that these properties are dominated by the exchange-repulsion and that the values of the exchange-repulsion contribution to the interaction-induced average polarizability drop upon decreasing the helium cage's radius.

2 | METHODOLOGY

In this communication the decomposition of the interaction energy was carried out using the scheme proposed by Mandado and Hermida-Ramón (density decomposition scheme, DDS),[73] which is based on the partitioning of the one-electron and exchange-correlation densities into unperturbed and deformation densities and allows for the representation of the interaction energy as a sum of physically well-defined electrostatic, exchange, repulsion and polarization terms. In this approach the interaction energy is expressed in terms of the unperturbed densities of the isolated subsystems and the deformation densities, which describe the effect (a) of the Pauli exclusion principle ($\Delta\rho_{Pauli}$) and (b) of the electron polarization due to the intermolecular interaction ($\Delta\rho_{Pol}$) on one-electron densities of monomers. DDS allows for the systematic definition of the components of energy at correlated levels of theory, and at the same time, in contrast to commonly used symmetry-adapted perturbation theory,[74] gives an insight into the electron density deformation due to the Pauli exclusion principle and polarization effects, providing three-dimensional pictures of interactions. The electrostatic and exchange energy terms of two interacting systems *A* and *B* are defined as follows:

$$E_{elec} = \int \hat{\nu}_{N_A}\rho_B\left(\vec{r}_1\right)d\vec{r}_1 + \int \hat{\nu}_{N_B}\rho_A\left(\vec{r}_1\right)d\vec{r}_1 + \int\int \frac{\rho_A\left(\vec{r}_1\right)\rho_B\left(\vec{r}_2\right)}{|\vec{r}_2-\vec{r}_1|}d\vec{r}_1 d\vec{r}_2 + \sum_{I=1}^{N_A}\sum_{J=1}^{N_B}\frac{Z_I Z_J}{|\vec{R}_I-\vec{R}_J|}, \quad (1)$$

$$E_{exch} = \frac{1}{2}\int\int \frac{\rho_{XC,AB}\left(\vec{r}_1,\vec{r}_2\right)}{|\vec{r}_2-\vec{r}_1|}d\vec{r}_1 d\vec{r}_2, \quad (2)$$

where ν_N, *N*, *Z* denote the electrostatic potential created by the nuclei, the number of nuclei and the nuclear charge, respectively, whereas $\vec{r}$ and $\vec{R}$ vectors describe the position of electrons and nuclei. $\rho\left(\vec{r}_1\right)$ and $\rho_{XC}\left(\vec{r}_1,\vec{r}_2\right)$ represent the one-electron density and the exchange-correlation density. The repulsion component is a function of the Pauli deformation density, which can be obtained using the weighted Lowdin's

orthogonalization procedure of the aggregate orbitals. In turn, the polarization energy is defined as a difference of the total interaction energy and a sum of electrostatic, exchange and repulsion terms. DDS was implemented in our in-house plugin to Psi4 quantum chemistry program.[75]

The calculations were performed for the LiH and HF molecules embedded in nanotube-like helium cages of decreasing diameter, i.e. (5,5)HeNT, (4,4)HeNT and (3,3)HeNT. The molecules were placed in the center of a helium nanotube along its main axis, which is the *z*-axis (see ref. [5] for details on the structure of the LiH@(n,n)HeNT and HF@(n,n)HeNT complexes). We also studied six model systems in which LiH is surrounded by various numbers of He atoms (see Figure 1 and ref. [9] for details). During the computations the MP2 (for LiH@(n,n)HeNT and HF@(n,n)HeNT complexes) and CCSD (for LiH-$(He)_n$ systems) methods in connection with Dunning's correlation consistent aug-cc-pVTZ basis set were used, all electrons were correlated and the studied complexes were divided into two fragments: guest molecule and helium environment.

The interaction-induced polarizability is defined as a difference between polarizability of the complex and the sum of polarizabilities of its noninteracting constituents. It can be evaluated as the derivative of interaction energy with respect to the electric field:

$$\Delta\alpha_{ij} = -\left(\frac{\partial^2 \Delta E_{int}}{\partial F_i \partial F_j}\right)_{F_i=F_j=0}. \tag{3}$$

In the same manner one can obtain the components of interaction-induced polarizability by replacing the interaction energy in the above equation with its respective component. It should be emphasized that in the present study the calculations were performed in the aggregate's basis set.

The interaction-induced polarizability and its electrostatic, exchange, repulsion and polarization components were evaluated in terms of the finite-field method using the corresponding energy terms and Romberg-Rutishauser extrapolation scheme.[76] In doing so, the electric field amplitudes $2^n h$, where h = 0.0002 a.u. and n = 0, 1, 7, were employed.

3 | RESULTS AND DISCUSSION

We will first look at the behavior of the interaction-induced polarizability of the LiH@(n,n)HeNT and HF@(n,n)HeNT complexes. As can be seen from Figure 2 the values of $\Delta\alpha_{zz,int}$, obtained herein using MP2 method and aug-cc-pVTZ basis set, systematically drop upon increasing the

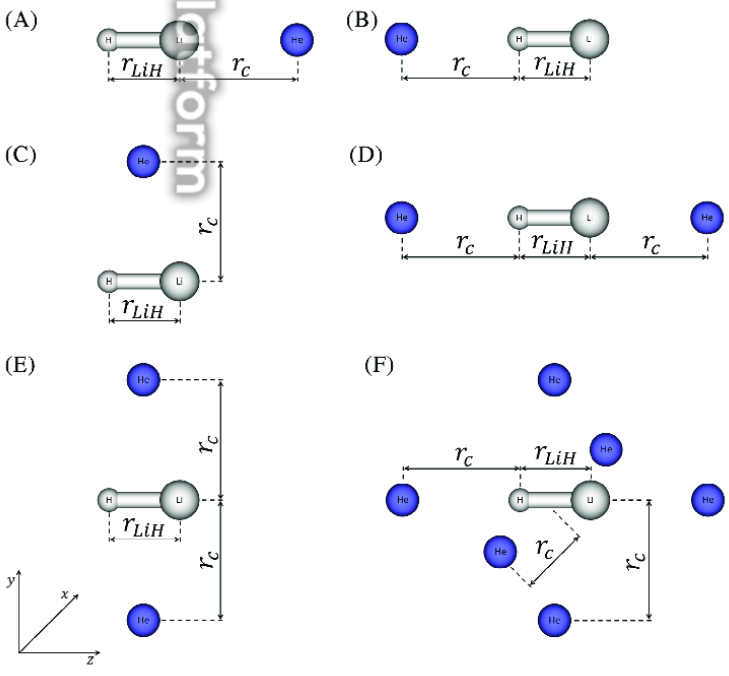

FIGURE 1 The LiH molecule surrounded by helium atoms. The r_{LiH} and r_c denote the LiH bond length (3.015 a.u.) and the distance between LiH and He, respectively. The He atoms oriented perpendicularly to the LiH molecule are positioned along the axis crossing the center of the LiH bond. The remaining He atoms are placed along the molecular axis of LiH. This figure is reprinted from ref. [9] with permission from Elsevier

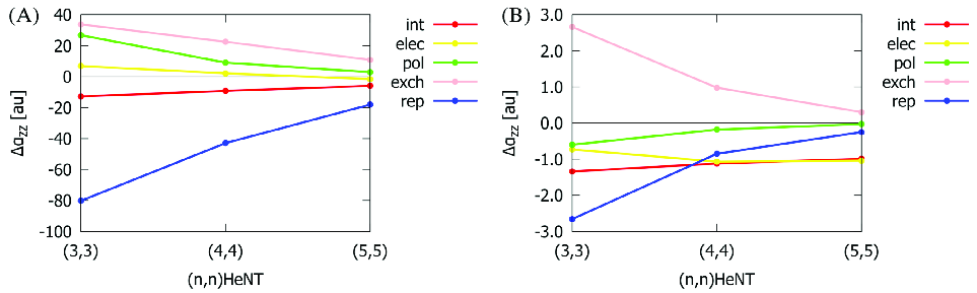

FIGURE 2 The interaction-induced polarizability and its electrostatic (elec), exchange (exch), repulsion (rep) and polarization (pol) components obtained for LiH@(n,n)HeNT (A) and HF@(n,n)HeNT (B) complexes at the MP2/aug-cc-pVTZ level of theory

(n,n)	α_{zz} (HF@(n,n)HeNT)	α_{zz} ((n,n)HeNT)	α'_{zz}((n,n)HeNT)	$\alpha_{zz,diff}$	$\alpha'_{zz,diff}$
	MP2/6-31G++(d,p)				
(3,3)	23.74	18.78	19.25	4.96	4.48
(4,4)	30.48	25.71	25.84	4.77	4.64
(5,5)	37.38	32.71	32.77	4.67	4.61
	MP2/aug-cc-pVTZ				
(3,3)	39.78	34.70	34.74	5.08	5.04
(4,4)	51.20	45.94	45.96	5.26	5.24
(5,5)	62.62	57.25	57.26	5.37	5.36

Note: All values are given in a.u.

TABLE 1 The values of total polarizability of HF@(n,n)HeNT aggregates (α_{zz}(HF(n,n)HeNT)), polarizability of empty helium nanotubes (α_{zz}((n,n)HeNT) and α'_{zz}((n,n)HeNT), where ' indicates that calculations were performed in aggregate's basis set) and the difference between polarizability of HF@(n,n)HeNTs and empty helium nanotubes ($\alpha_{zz,diff}$ = α_{zz}(HF@(n,n)HeNT)-α_{zz}((n,n)HeNT) and $\alpha'_{zz,diff}$ = α_{zz}(HF@(n,n)HeNT)-α'_{zz}((n,n)HeNT))

strength of spatial confinement (i.e. decreasing the nanotube's diameter). As mentioned in the Introduction section, $\alpha_{zz,diff}$ calculated previously at the MP2/6-31++G(d,p) level of theory for the same HF@(n,n)HeNT systems, exhibits a growing trend.[5] Hence, let us compare two quantities: $\alpha_{zz,diff}$ = α_{zz}(HF@(n,n)HeNT)−α_{zz}((n,n)HeNT) and $\alpha'_{zz,diff}$ = α_{zz} (HF@(n,n)HeNT)−α'_{zz}((n,n)HeNT) = $\Delta\alpha_{zz,int}$ + α'_{zz} (HF), where α'_{zz} ((n,n)HeNT) and α'_{zz} (HF) were calculated in aggregate's basis set, obtained at the MP2/6-31++G(d,p) and MP2/aug-cc-pVTZ level of theory (see Table 1). As can be seen, eliminating the basis set superposition error from the calculations performed at the MP2/6-31++G(d,p) level changes the behavior of polarizability, which becomes nonmonotonic (see $\alpha'_{zz,diff}$ in Table 1). However, when aug-cc-pVTZ basis set is used both $\alpha_{zz,diff}$ and $\alpha'_{zz,diff}$ decrease together with increasing the strength of spatial confinement. Therefore, it is clear that the source of the previously reported unexpected growth of the polarizability of HF embedded in helium nanotubes lays in the applied methodology.

We will now analyze the repulsion component of the interaction-induced polarizability ($\Delta\alpha_{zz,rep}$) of the LiH@(n,n)HeNT and HF@(n,n)HeNT complexes and compare it with the total polarizability, calculated previously in the presence of cylindrically symmetric harmonic oscillator potential,[5] which represents pure electron repulsion effect. The data presented in Figure 2 show that increasing the strength of spatial confinement leads to a decrease of the repulsion component of the interaction-induced polarizability of LiH and HF embedded in helium nanotubes. In the case of LiH@(n,n)HeNT complexes there is a quite significant drop in value of $\Delta\alpha_{zz,rep}$ by around 60 a.u. On the other hand, the quantitative changes of $\Delta\alpha_{zz,rep}$ of HF@(n,n)HeNTs are much smaller compared with the ones observed for LiH@(n,n)HeNTs. The behavior of $\Delta\alpha_{zz,rep}$ of LiH@(n,n)HeNT and HF@(n,n)HeNT systems is consistent with the behavior of the total polarizability of LiH and HF embedded in cylindrically symmetric harmonic oscillator potential, which diminishes upon increasing the strength of spatial confinement (see Figures 7a and 9a in ref. [5]).

Let us now look at the other components and their contribution to the interaction-induced polarizability. In the case of LiH@(n,n)HeNTs the exchange, electrostatic and polarization components of $\Delta\alpha_{zz,int}$, in contrast to the repulsion term, rise together with a diminishment of helium nanotube's diameter. It is also worth noticing that in comparison to other components the changes of $\Delta\alpha_{zz,elec}$ are very small. Moreover, the transition between LiH@(5,5)HeNT and LiH@(4,4)HeNT is accompanied by the change in sign of $\Delta\alpha_{zz,elec}$. It is clear from Figure 2A that the interaction-induced polarizability of the LiH@(n,n)HeNT systems is strongly dominated by the repulsion component. Similarly as in the case of LiH@(n,n)HeNTs, the exchange component of $\Delta\alpha_{zz,int}$ of HF@(n,n)HeNTs grows upon increasing the pressure exerted on HF by the helium nanotubes (see Figure 2B). On the other hand, one can observe a diminishment of $\Delta\alpha_{zz,pol}$ and nonmonotonic behavior of $\Delta\alpha_{zz,elec}$. Among all four terms $\Delta\alpha_{zz,elec}$ contributes the most to the interaction-induced polarizability of HF@(4,4)HeNT and HF@(5,5)HeNT. In turn, in the case of HF@(3,3)HeNT the repulsion and exchange terms prevail and, due to a difference in sign, they cancel each other out.

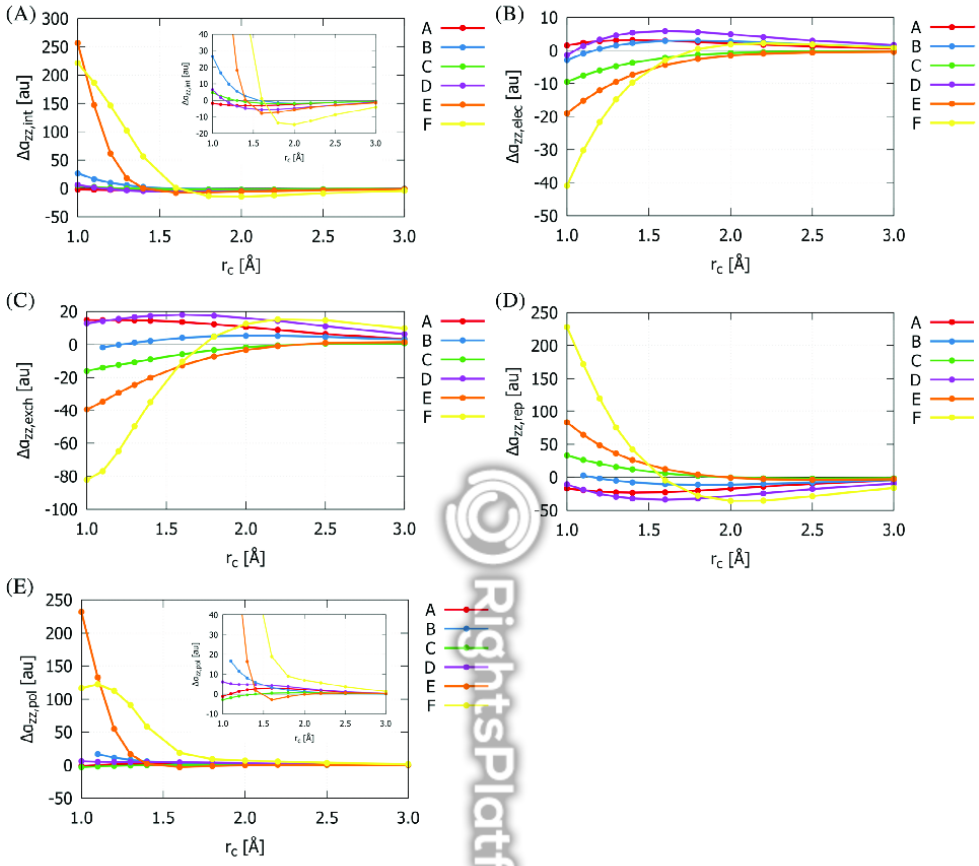

FIGURE 3 The interaction-induced polarizability (A) and its electrostatic (B), exchange (C), repulsion (D) and polarization (E) components obtained for LiH-$(He)_n$ complexes at the CCSD/aug-cc-pVTZ level of theory. Note that the missing points on the graphs are due to the numerical instabilities of the results

We will now consider the effect of non-isotropic alignment of confining species in the LiH-$(He)_n$ complexes on the interaction-induced polarizability. The $\Delta\alpha_{zz,int}$ of the analyzed LiH-$(He)_n$ systems exhibits nonmonotonic behavior (see Figure 3). Together with increasing the orbital compression strength the values of $\Delta\alpha_{zz,int}$ initially decrease and then they rise. The most significant increase is observed for models E and F, as the values of $\Delta\alpha_{zz,int}$ for the LiH-He distance equal to 1.0 Å reach 256.44 and 221.19 a.u., respectively. The changes of $\Delta\alpha_{zz,int}$ of the remaining complexes are much smaller, especially in the case of systems A, C and D. Interestingly, when one He atom is located along the LiH bond on the hydrogen side (model B) there is a quite significant, although not that large as for systems E and F, increase of $\Delta\alpha_{zz,int}$. In turn, adding another He atom on the opposite side (model D) causes a notable reduction of $\Delta\alpha_{zz,int}$ values, however, the nonmonotonic behavior of $\Delta\alpha_{zz,int}$ is preserved.

The data presented in Figure 3 show that the behavior of the repulsion term is very similar to the behavior of the interaction-induced polarizability of the LiH-$(He)_n$ complexes. Initially, $\Delta\alpha_{zz,rep}$ decreases as a result of shortening the distance between LiH and He, which is in line with the behavior of the total polarizability of LiH embedded in confining potential. However, for each complex there is a point where this trend changes and $\Delta\alpha_{zz,rep}$ starts to grow. In most cases a diminishment of $\Delta\alpha_{zz,rep}$ is observed for LiH-He distances ranging from 3 Å to at least 2 Å. However, for systems C and E a decrease of $\Delta\alpha_{zz,rep}$ occurs only in the region of LiH-He distances between 3 and 2.5 Å. The most significant rise of $\Delta\alpha_{zz,rep}$ is observed in the region of great spatial confinement strength for models with at least two helium atoms placed perpendicularly to the LiH bond (E and F). The character of changes of the exchange, electrostatic and polarization components of the interaction-induced polarizability of LiH-$(He)_n$ systems depends on the complex in question, however, the most pronounced changes of these three terms are observed for systems E and F. In contrast to $\Delta\alpha_{zz,rep}$, in the strong orbital compression region there is a systematic drop of $\Delta\alpha_{zz,elec}$ and $\Delta\alpha_{zz,exch}$ values. In turn, when LiH-He

distances are small, $\Delta\alpha_{zz,pol}$ of models A and C decreases, whereas in the case of remaining models a rise of $\Delta\alpha_{zz,pol}$ occurs. It should also not be overlooked that the reduction of LiH-He distance from 1.1 to 1.0 Å is accompanied by a slight decrease of $\Delta\alpha_{zz,pol}$ of the three-dimensional system F. In most cases the repulsion component has prevalent contribution to the interaction-induced polarizability of the LiH-$(He)_n$ complexes.

In order to obtain more insight into the origins of the behavior of polarizability upon confinement, we have plotted the Pauli and polarization deformation densities for the studied complexes (see Figures 4-6). As can be seen, in all considered LiH@(n,n)HeNT and HF@(n,n)HeNT systems an inward flow of the Pauli density towards the guest molecule occurs, leading to the net decrease of the spatial extent of electron density, i.e. to the decrease of total polarizability. In contrast, density change due to polarization effects is delocalized over whole complexes and its influence on the electron density extent is more complicated. It is interesting to note that in the case of systems A-F (Figure 6), which have much less confining bodies than the caged clusters, $\Delta\rho_{Pauli}$ leaks from the guest molecules into the environment. It is due to the high degree of density redistribution within the helium atoms upon antisymmetrization of the Hartree product of unperturbed molecules. In this case, the effect of the Pauli repulsion wall on polarizability depends on the geometry of confinement and causes a decrease of $\Delta\alpha_{zz,rep}$ in most cases, with exceptional increase of $\Delta\alpha_{zz,rep}$ in the strong orbital overlap region (see scans in Figure 3D and maps for r_c = 1.2 Å in Figure 6).

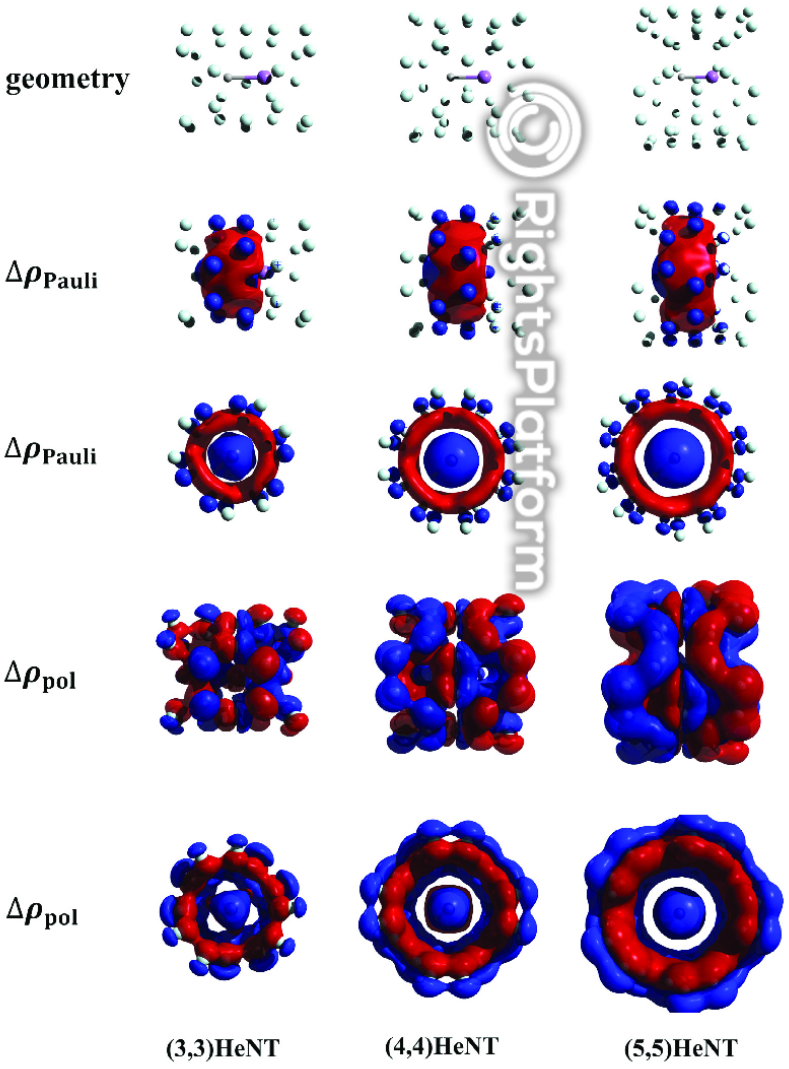

FIGURE 4 The $\Delta\rho_{Pauli}$ and $\Delta\rho_{pol}$ deformation densities obtained at the MP2/aug-cc-pVTZ level of theory using DDS method for LiH@(n,n)HeNT complexes (two views are presented: side view and a view along the main axis of a nanotube). The 0.0004, 0.0001 and 0.00002 isosurface values were used for LiH@(3,3)HeNT, LiH@(4,4)HeNT and LiH@(5,5) HeNT, respectively. Blue (red) denotes spaces where density increases (decreases). The plots were obtained using Avogadro program[77,78]

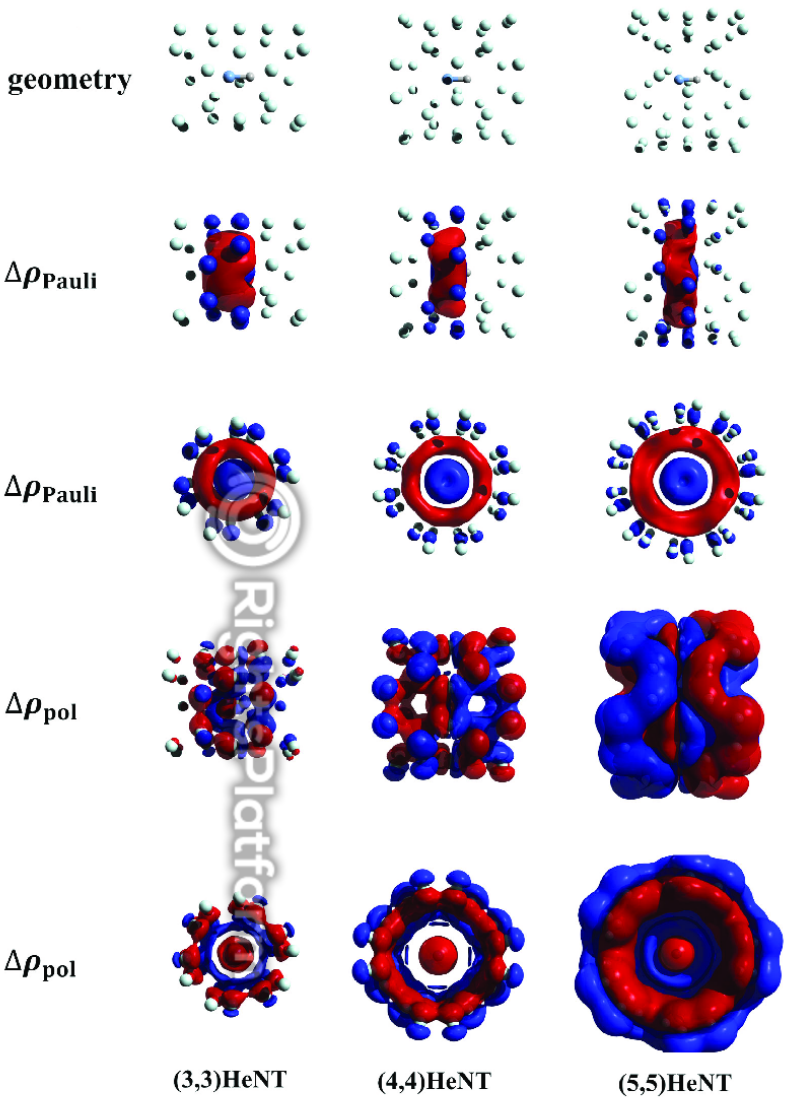

FIGURE 5 The $\Delta\rho_{Pauli}$ and $\Delta\rho_{pol}$ deformation densities obtained at the MP2/aug-cc-pVTZ level of theory using DDS method for HF@(n,n)HeNT complexes (two views are presented: side view and a view along the main axis of a nanotube). The 0.0003, 0.00005 and 0.000004 isosurface values were used for HF@(3,3)HeNT, HF@(4,4)HeNT and HF@(5,5) HeNT, respectively. Blue (red) denotes spaces where density increases (decreases). The plots were obtained using Avogadro program[77,78]

4 | CONCLUSIONS

In order to analyze the correspondence between the two forms of spatial confinement, i.e. the real chemical environment and the repulsive analytical potential, which describes only pure electronic compression, we performed a decomposition of the interaction-induced polarizability of the LiH and HF molecules in various helium environments into electrostatic, exchange, repulsion and polarization contributions. In doing so, we were especially interested in comparing the repulsion effects of the confining helium environment to these represented by the external repulsive potentials (like the cylindrically symmetric harmonic oscillator potential). Based on the conducted research we observed that the increase of the pressure exerted by the nanotube-like helium cages on the LiH and HF molecules leads to a diminishment of the repulsion component of the interaction-induced polarizability. It is in line with the behavior of the total polarizability of LiH, HF and other atoms and molecules embedded in repulsive potentials upon increasing the strength of spatial confinement. The behavior of the repulsion term of most of the LiH-$(He)_n$ complexes matches the trends observed for LiH and HF embedded in helium nanotubes, as the radius of the smallest nanotube (which is (3,3)HeNT) equals

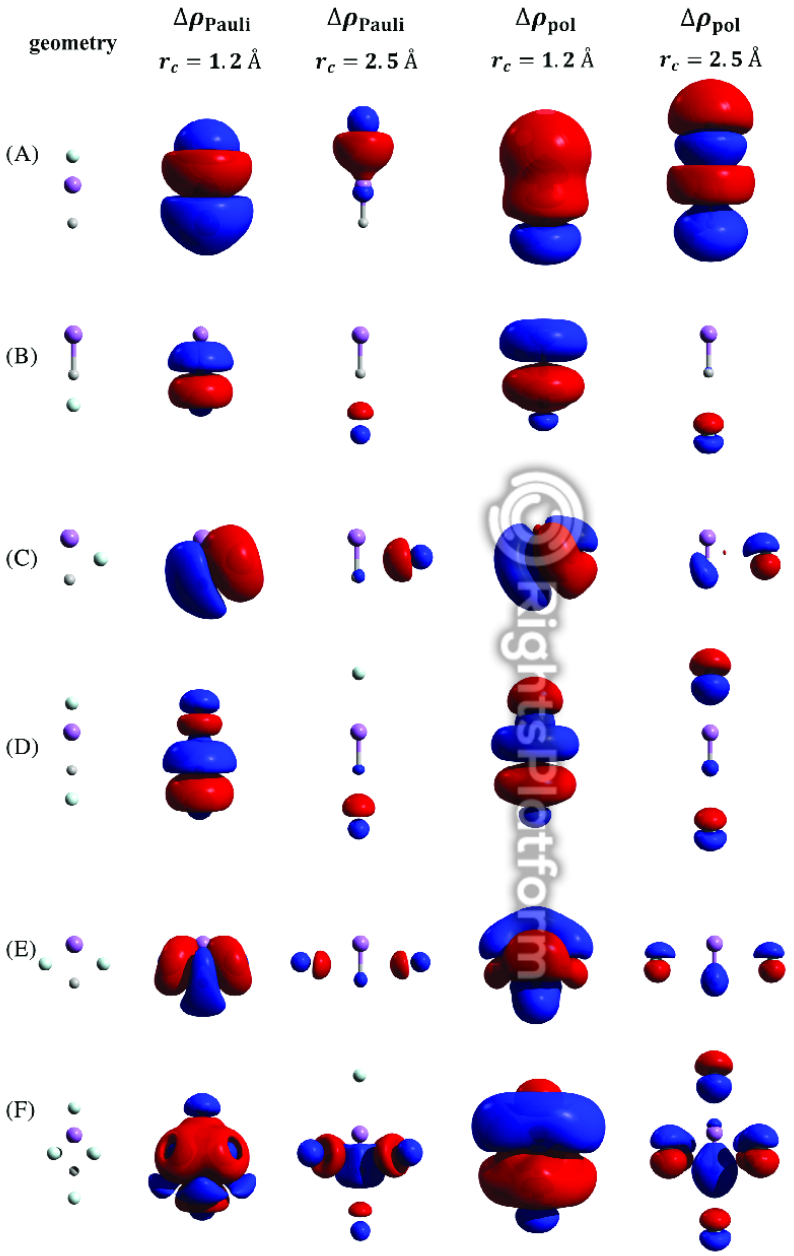

FIGURE 6 The $\Delta\rho_{\mathrm{Pauli}}$ and $\Delta\rho_{\mathrm{pol}}$ deformation densities obtained at the CCSD/aug-cc-pVTZ level of theory using DDS method for LiH-$(He)_n$ systems with two selected LiH-He distances (denoted as r_c). The 0.000003, 0.0002, 0.0002, 0.00015, 0.00035, 0.0002 isosurface values were used for models A, B, C, D, E and F, respectively. Blue (red) denotes spaces where density increases (decreases). The plots were obtained using Avogadro program[77,78]

2.1 Å and in the region of LiH-He distances between 3 and 2.1 Å the values of $\Delta\alpha_{zz,rep}$ of almost all LiH-$(He)_n$ systems, except C and E, similarly as of LiH@(n,n)HeNTs and HF@(n,n)HeNTs, decrease. In general, a decrease of $\Delta\alpha_{zz,rep}$, caused by increasing the strength of spatial confinement, was observed for all complexes studied herein. However, the region of orbital compression strengths, in which this decrease occurs, is different for each system.

ACKNOWLEDGMENTS

This project is carried out under POLONEZ programme which has received funding from the European Union's Horizon 2020 research and innovation programme under the Marie Skłodowska-Curie grant agreement No. 665778. This project is funded by National Science Centre, Poland (grant no. 2016/23/P/ST4/01720) within the POLONEZ 3 fellowship.

This work was supported by Wrocław University of Science and Technology. The authors gratefully acknowledge Wroclaw Centre for Networking and Supercomputing for the generous allotment of computer time.

We cordially thank Professor Marcos Mandado from Universidade de Vigo in Spain for providing us with his benchmark calculations to validate our implementation of the DDS method.

AUTHOR CONTRIBUTIONS

Marta Choluj: Conceptualization; data curation; formal analysis; investigation; methodology; validation; visualization; writing-original draft; writing-review and editing. **Bartosz Blasiak:** Conceptualization; formal analysis; funding acquisition; investigation; methodology; software; writing-review and editing. **Wojciech Bartkowiak:** Conceptualization; formal analysis; project administration; supervision; writing-review and editing.

ORCID

Marta Chołuj https://orcid.org/0000-0003-2461-4851
Bartosz Błasiak https://orcid.org/0000-0003-1968-3465
Wojciech Bartkowiak https://orcid.org/0000-0002-3442-9302

REFERENCES

[1] W. Jaskólski, *Phys. Rep*. **1996**, *27*, 1.
[2] J. R. Sabin, E. Brändas, S. A. Cruz Eds., *Advances in Quantum Chemistry: Theory of Confined Quantum Systems*, Vol. 57-58, Academic Press, Waltham, MA **2009**.
[3] K. D. Sen Ed., *Electronic Structure of Quantum Confined Atoms and Molecules*, Springer International Publishing, Switzerland **2014**.
[4] D. A. Britz, A. N. Khlobystov, *Chem. Soc. Rev*. **2006**, *35*, 637.
[5] J. Kozłowska, R. Zaleśny, W. Bartkowiak, *Chem. Phys*. **2014**, *428*, 19.
[6] N. A. Besley, A. Noble, *J. Chem. Phys*. **2008**, *128*, 101102.
[7] G. García, I. Ciofini, M. Fernández-Gómez, *J. Phys. Chem. Lett*. **2013**, *4*, 1239.
[8] A. Kaczmarek, W. Bartkowiak, *Phys. Chem. Chem. Phys*. **2009**, *11*, 2885.
[9] M. Chołuj, J. Kozłowska, A. Roztoczyńska, W. Bartkowiak, *Chem. Phys*. **2015**, *459*, 24.
[10] A. Kaczmarek, R. Zaleśny, W. Bartkowiak, *Chem. Phys. Lett*. **2007**, *449*, 314.
[11] A. Kaczmarek-Kedziera, *J. Phys. Chem. A* **2011**, *115*, 5210.
[12] M. G. Papadopoulos, A. J. Sadlej, *Chem. Phys. Lett*. **1998**, *288*, 377.
[13] O. Shameema, C. N. Ramachandran, N. Sathyamurthy, *J. Phys. Chem. A* **2006**, *110*, 2.
[14] D. Kedziera, A. Avramopoulos, M. G. Papadopoulos, A. J. Sadlej, *Phys. Chem. Chem. Phys*. **2003**, *5*, 1096.
[15] J. Karwowski, *J. Mol. Struct. Theochem*. **2005**, *727*, 1.
[16] R. W. Góra, R. Zaleśny, J. Kozłowska, P. Naciazek, A. Roztoczyńska, K. Strasburger, W. Bartkowiak, *J. Chem. Phys*. **2012**, *137*, 094307.
[17] J. M. H. Lo, M. Klobukowski, G. H. F. Diercksen, in *Advances in Quantum Chemistry*, Vol. 48 (Ed: J. R. Sabin), Academic Press, Waltham, MA **2005**, p. 59.
[18] W. Bartkowiak, K. Strasburger, *J. Mol. Struc. Theochem*. **2010**, *960*, 93.
[19] D. Bielińska-Waż, J. Karwowski, G. H. F. Diercksen, *J. Phys. B: At., Mol. Opt. Phys*. **2001**, *34*, 1987.
[20] K. Strasburger, P. Naciążek, *J. Phys. B: At., Mol. Opt. Phys*. **2014**, *47*, 025002.
[21] R. LeSar, D. R. Herschbach, *J. Phys. Chem*. **1983**, *87*, 5202.
[22] J. Gorecki, W. B. Brown, *J. Chem. Phys*. **1988**, *89*, 2138.
[23] T. Sako, G. H. F. Diercksen, *J. Phys. B: At., Mol. Opt. Phys*. **2003**, *36*, 3743.
[24] R. Zaleśny, R. W. Góra, J. Kozłowska, J. M. Luis, H. Ågren, W. Bartkowiak, *J. Chem. Theory Comput*. **2013**, *9*, 3463.
[25] A. Sarsa, C. L. Sech, *J. Phys. B: At., Mol. Opt. Phys*. **2012**, *45*, 205101.
[26] J. Tomasi, B. Mennucci, R. Cammi, *Chem. Rev*. **2005**, *105*, 2999.
[27] R. Cammi, V. Verdolino, B. Mennucci, J. Tomasi, *Chem. Phys*. **2008**, *344*, 135.
[28] R. Cammi, C. Cappelli, B. Mennucci, J. Tomasi, *J. Chem. Phys*. **2012**, *137*, 154112.
[29] M. Pagliai, G. Cardini, R. Cammi, *J. Phys. Chem. A* **2014**, *118*, 5098.
[30] A. L. Buchachenko, *J. Phys. Chem. B* **2001**, *105*, 5839.
[31] A. K. Roy, *Int. J. Quant. Chem*. **2015**, *115*, 937.
[32] H. E. Montgomery Jr., N. Aquino, A. Flores-Riveros, *Phys. Lett. A* **2010**, *374*, 2044.
[33] H. E. Montgomery Jr., V. I. Pupyshev, *Theor. Chem. Acc*. **2015**, *134*, 1598.
[34] H. E. Montgomery Jr., *Eur. J. Phys*. **2011**, *32*, 1275.
[35] L. Stevanović, K. D. Sen, *J. Phys. B: At., Mol. Opt. Phys*. **2008**, *41*, 205002.
[36] A. Sarsa, E. Buendia, F. J. Gálvez, *J. Phys. B: At., Mol. Opt. Phys*. **2014**, *47*, 185002.
[37] D. Bielińska-Wąż, G. H. F. Diercksen, M. Klobukowski, *Chem. Phys. Lett*. **2001**, *349*, 215.

[38] A. Borgoo, D. J. Tozer, P. Geerlings, F. D. Proft, *Phys. Chem. Chem. Phys.* **2008**, *10*, 1406.
[39] A. Borgoo, D. J. Tozer, P. Geerlings, F. D. Proft, *Phys. Chem. Chem. Phys.* **2009**, *11*, 2862.
[40] A. Sommerfeld, H. Welker, *Ann. Phys.* **1938**, *424*, 56.
[41] R. B. Dingle, *Proc. Camb. Phil. Soc.* **1953**, *49*, 103.
[42] Y. P. Varshni, *J. Phys. B: At., Mol. Opt. Phys* **1998**, *31*, 2849.
[43] A. Banerjee, K. D. Sen, J. Garza, R. Vargas, *J. Chem. Phys.* **2002**, *116*, 4054.
[44] E. Ley-Koo, S. Rubinstein, *J. Chem. Phys.* **1979**, *71*, 351.
[45] J. M. H. Lo, M. Klobukowski, *Chem. Phys.* **2006**, *328*, 132.
[46] R. Zaleśny, R. W. Góra, J. M. Luis, W. Bartkowiak, *Phys. Chem. Chem. Phys.* **2015**, *17*, 21782.
[47] A. Roztoczyńska, J. Kozłowska, P. Lipkowski, W. Bartkowiak, *Chem. Phys. Lett.* **2014**, *608*, 264.
[48] S. Sen, P. Mandal, P. K. Mukherjee, *Phys. Plasmas* **2012**, *19*, 033501.
[49] N. Aquino, G. Campoy, H. E. Montgomery, *Int. J. Quantum Chem.* **2007**, *107*, 1548.
[50] S. Mateos-Cortés, E. Ley-Koo, S. A. Cruz, *Int. J. Quantum Chem.* **2002**, *86*, 376.
[51] F. Holka, P. Neogrády, V. Kellö, M. Urban, G. H. F. Diercksen, *Mol. Phys.* **2005**, *103*, 2747.
[52] F. Holka, M. Urban, P. Neogrády, J. Paldus, *J. Chem. Phys.* **2014**, *141*, 214303.
[53] M. Chołuj, W. Bartkowiak, *Chem. Phys. Lett.* **2016**, *663*, 84.
[54] J. Kozłowska, W. Bartkowiak, *Chem. Phys.* **2014**, *441*, 83.
[55] J. Kozłowska, A. Roztoczyńska, W. Bartkowiak, *Chem. Phys.* **2015**, *456*, 98.
[56] M. Chołuj, J. Kozłowska, W. Bartkowiak, *Int. J. Quantum Chem.* **2018**, *118*, e25666.
[57] R. Zaleśny, M. Chołuj, J. Kozłowska, W. Bartkowiak, J. M. Luis, *Phys. Chem. Chem. Phys.* **2017**, *19*, 24276.
[58] M. Chołuj, W. Bartkowiak, P. Naciążek, K. Strasburger, *J. Chem. Phys.* **2017**, *146*, 194301.
[59] J. Kozłowska, M. Chołuj, R. Zaleśny, W. Bartkowiak, *Phys. Chem. Chem. Phys.* **2017**, *19*, 7568.
[60] P. W. Fowler, A. J. Sadlej, *Mol. Phys.* **1992**, *77*, 709.
[61] P. W. Fowler, K. L. C. Hunt, H. M. Kelly, A. J. Sadlej, *J. Chem. Phys.* **1994**, *100*, 2932.
[62] R. Moszyński, T. G. A. Heijmen, P. E. S. Wormer, A. van der Avoird, *J. Chem. Phys.* **1996**, *104*, 6997.
[63] T. G. A. HeijmenN, P. E. S. W. Robert Moszyński, A. van der Avoird, *Mol. Phys.* **1996**, *89*, 81.
[64] G. Maroulis, *J. Phys. Chem. A* **2000**, *104*, 4772.
[65] J. López Cacheiro, B. Fernández, D. Marchesan, S. Coriani, C. Hättig, A. Rizzo, *Mol. Phys.* **2004**, *102*, 101.
[66] B. Skwara, W. Bartkowiak, A. Zawada, R. W. Góra, J. Leszczyński, *Chem. Phys. Lett.* **2007**, *436*, 116.
[67] B. Skwara, A. Kaczmarek, R. W. Góra, W. Bartkowiak, *Chem. Phys. Lett.* **2008**, *461*, 203.
[68] A. Baranowska, B. Fernández, A. Rizzo, B. Jansík, *Phys. Chem. Chem. Phys.* **2009**, *11*, 9871.
[69] R. W. Góra, R. Zaleśny, A. Zawada, W. Bartkowiak, B. Skwara, M. G. Papadopoulos, D. L. Silva, *J. Phys. Chem. A* **2011**, *115*, 4691.
[70] A. Zawada, M. M. R. W. Góra, M. M. Mikołajczyk, W. Bartkowiak, *J. Phys. Chem. A* **2012**, *116*, 4409.
[71] R. W. Góra, B. Błasiak, *J. Phys. Chem. A* **2013**, *117*, 6859.
[72] R. Zaleśny, M. Medved, R. W. Góra, H. Reis, J. M. Luis, *Phys. Chem. Chem. Phys.* **2018**, *20*, 19841.
[73] M. Mandado, J. M. Hermida-Ramón, *J. Chem. Theory Comput.* **2011**, *7*, 633.
[74] B. Jeziorski, R. Moszyński, K. Szalewicz, *Chem. Rev.* **1994**, *94*, 1887.
[75] R. M. Parrish, L. A. Burns, D. G. A. Smith, A. C. Simmonett, A. E. DePrince III., E. G. Hohenstein, U. Bozkaya, A. Y. Sokolov, R. Di Remigio, R. M. Richard, et al., *J. Chem. Theory Comput.* **2017**, *13*, 3185.
[76] M. Medved, M. Stachovà, D. Jacquemin, J. M. Andrè, E. A. Perpeté, *J. Mol. Struc. Theochem.* **2007**, *847*, 39.
[77] Avogadro: An open-source molecular builder and visualization tool. Version 1.2.0, http://avogadro.cc/ (accessed: May 2020).
[78] M. D. Hanwell, D. E. Curtis, D. C. Lonie, T. Vandermeersch, E. Zurek, G. R. Hutchison, *Aust. J. Chem.* **2012**, *4*, 1.

How to cite this article: Chołuj M, Błasiak B, Bartkowiak W. Partitioning of the interaction-induced polarizability of molecules in helium environments. *Int J Quantum Chem*. 2021;121:e26544. https://doi.org/10.1002/qua.26544